Acta Pharmacologica Sinica

www.nature.com/aps

ARTICLE

Targeted VEGFA therapy in regulating early acute kidney injury and late fibrosis

Meng-jie Huang[1], Yu-wei Ji[1], Jian-wen Chen[1], Duo Li[2], Tian Zhou[3], Peng Qi[4], Xu Wang[1], Xiao-fan Li[1], Yi-fan Zhang[1], Xiang Yu[1], Ling-ling Wu[1], Xue-feng Sun[1], Guang-yan Cai[1], Xiang-mei Chen[1], Quan Hong[1]✉ and Zhe Feng[1]✉

Damage to peritubular capillaries is a key process that contributes to acute kidney injury (AKI) progression. Vascular endothelial growth factor A (VEGFA) plays a critical role in maintaining the renal microvasculature. However, the physiological role of VEGFA in various AKI durations remains unclear. A severe unilateral ischemia–reperfusion injury model was established to provide an overview of VEGFA expression and the peritubular microvascular density from acute to chronic injury in mouse kidneys. Therapeutic strategies involving early VEGFA supplementation protecting against acute injury and late anti-VEGFA treatment for fibrosis alleviation were analyzed. A proteomic analysis was conducted to determine the potential mechanism of renal fibrosis alleviation by anti-VEGFA. The results showed that two peaks of extraglomerular VEGFA expression were observed during AKI progression: one occurred at the early phase of AKI, and the other occurred during the transition to chronic kidney disease (CKD). Capillary rarefaction progressed despite the high expression of VEGFA at the CKD stage, and VEGFA was associated with interstitial fibrosis. Early VEGFA supplementation protected against renal injury by preserving microvessel structures and counteracting secondary tubular hypoxic insults, whereas late anti-VEGFA treatment attenuated renal fibrosis progression. The proteomic analysis highlighted an array of biological processes related to fibrosis alleviation by anti-VEGFA, which included regulation of supramolecular fiber organization, cell-matrix adhesion, fibroblast migration, and vasculogenesis. These findings establish the landscape of VEGFA expression and its dual roles during AKI progression, which provides the possibility for the orderly regulation of VEGFA to alleviate early acute injury and late fibrosis.

Keywords: vascular endothelial growth factor; kidney; fibrosis

Acta Pharmacologica Sinica (2023) 44:1815–1825; https://doi.org/10.1038/s41401-023-01070-1

INTRODUCTION

Acute kidney injury (AKI) is a common and severe syndrome that is characterized by a rapid decline in renal function and is associated with increasing incidence and high mortality rates [1]. In surviving patients, renal function is generally expected to recover. However, persistent or severe injury can result in the failure of renal repair and the transition to chronic kidney disease (CKD) [2]. It is estimated that the prevalence of CKD is over 10% of the general population worldwide, amounting to >800 million individuals [3, 4]. These patients have an increased risk for end-stage renal disease, cardiovascular disease, and death [5, 6]. The high morbidity and adverse prognosis greatly burden public health systems.

The kidney is permeated by a highly complex vascular system with glomerular and peritubular capillary networks that are essential for maintaining the normal functions of the kidneys by delivering oxygen and nutrients [7]. The development of functional and structural abnormalities in the renal microvasculature that result in hypoxia is a key process that contributes to the pathophysiology of AKI progression [8]. Vascular endothelial growth factor A isoform (VEGFA), which is a proliferative survival factor for endothelial cells, plays a central role in promoting angiogenesis. Extraglomerular VEGFA mostly localizes in tubules under normal physiological conditions and is increased under hypoxic conditions. However, the regulation and physiological roles of VEGFA in different settings and various AKI timepoints appear multifaceted and complex. In some studies, the VEGFA levels were found to be significantly elevated 24 h after ischemic insult [9, 10] and then trended to decrease to the baseline at 72–96 h [11]. Basile et al reported a sustained high level of renal VEGFA during AKI progression [12]. The expression of VEGFA in the kidney during the transition from AKI to CKD has varied widely across studies [13, 14]. The inconsistency of renal VEGFA expression at different timepoints results in a lack of a clear understanding of its expression patterns.

Many studies have demonstrated that VEGFA contributes to AKI outcomes. However, whether VEGFA is protective or detrimental has not yet been clearly answered. In some preclinical models of ischemic AKI, treatment with exogenous VEGF shows therapeutic efficacy by reducing capillary rarefaction and inhibiting neutrophil

[1]Department of Nephrology, First Medical Center of Chinese PLA General Hospital, Nephrology Institute of the Chinese People's Liberation Army, State Key Laboratory of Kidney Diseases, National Clinical Research Center for Kidney Diseases, Beijing Key Laboratory of Kidney Disease Research, Beijing 100853, China; [2]Institute of Disaster and Emergency Medicine, Tianjin University, Tianjin 300072, China; [3]The Second Affiliated Hospital of Guizhou University of Traditional Chinese Medicine, Guiyang 550003, China and [4]Department of Emergency, First Medical Center of Chinese PLA General Hospital, Beijing 100853, China
Correspondence: Quan Hong (redhq@163.com) or Zhe Feng (zhezhe_4025@126.com)
These authors contributed equally: Meng-jie Huang, Yu-wei Ji, Jian-wen Chen

Received: 19 August 2022 Accepted: 22 February 2023
Published online: 13 April 2023

accumulation and leukocyte adhesion [14–16]. However, Xu et al. showed that inhibition of VEGFA expression prevents AKI by reducing inflammation and oxidative stress [17]. In addition, although some studies have shown that VEGFA promotes fibrogenesis in other organ systems [18–21] and that anti-VEGF therapy can significantly improve the therapeutic effects on liver fibrosis and pulmonary fibrosis [22, 23], there remain controversies about the profibrotic and antifibrotic effects of VEGFA in progressive kidney diseases [24, 25]. Thus, strategies that target this factor in the treatment of AKI often result in inconsistent outcomes. These perplexing findings prompted us to revisit the molecular characterization of VEGFA in AKI progression.

In this study, we established a severe unilateral ischemia–reperfusion injury (UIRI) model that is characterized by evident fibrosis to provide an overview of VEGFA expression from acute to chronic injury in mouse kidneys. We aimed to elucidate the characteristics and pathophysiological effects of extraglomerular VEGFA at different phases of AKI and to identify a targeted therapeutic approach based on an understanding of these mechanisms. We propose that VEGFA plays dual roles in early acute injury and late fibrosis. Transient VEGFA expression is necessary to preserve the renal microvessel structure at the early phase of AKI, whereas increased or prolonged expression of this factor at the late phase triggers maladaptive responses, leading to the development of renal fibrosis.

MATERIALS AND METHODS

Animal models and exogenous VEGFA supplementation/anti-VEGF therapy

Wild-type male C57BL/6 mice (aged 8 weeks) were raised in a specific pathogen-free facility at the Animal Center of Chinese PLA General Hospital. For the UIRI model, the unilateral renal pedicles (left) of the mice were clipped for 28 min with microaneurysm clamps. During the ischemic period, the core body temperature was monitored and maintained at 37 °C using a temperature-controlled heating system. A delayed contralateral nephrectomy (right kidney) was performed 1 day before sample harvest [26–28]. This UIRI model could induce kidney injury of notable severity without a high mortality rate, permitting an assessment of AKI-to-CKD progression.

VEGF164 (HY-P7421, MedChemExpress, USA) was diluted in 0.9% NaCl as a vehicle and was intravenously administered to mice at a dose of 100 μg/kg every day through two daily injections, with the first administration beginning at the time of reperfusion. The mice were intravenously injected with a well-characterized VEGFA-neutralizing antibody (512810, BioLegend, USA) at a dose of 100 μg per mouse ×2/week from day 7 to day 14 after AKI. Vehicle-treated mice served as controls.

Histopathological examination and immunohistochemical staining

Kidney tissue was fixed in 4% formaldehyde, dehydrated, and embedded in paraffin. Tissue sections (2 μm) were stained with hematoxylin-eosin (HE), periodic acid-Schiff (PAS), and Masson's trichrome. Tubular injury was assessed using the PAS-stained sections in a blinded manner and was described using the acute tubular necrosis (ATN) scores, as reflected by grades of tubular necrosis, cast formation, tubular dilation, and loss of brush borders. Ten nonoverlapping fields (200×) were randomly selected at the cortical medullary junction area and scored from 0 to 4 (0: normal; 1: mild to moderate injury, 1%–25% involvement; 2: severe injury, 26%–49% involvement; 3: high severe injury, involvement of 50%–75%; and 4: extensive injury, >75% involvement).

Immunohistochemical staining (IHC) was performed as described previously [29]. Tissues were labeled with anti-VEGFA (1:200, ab52917, Abcam, UK) and anti-endomucin (1:200, sc-65495, Santa Cruz, USA). To quantify the microvasculature in kidneys, Endomucin+ glomeruli were manually excluded from the images. All tissue evaluations were performed in a blinded manner.

Multiplex fluorescent IHC

Multiplex fluorescent IHC staining was conducted using Opal 7-Color Manual IHC Kits (NEL811001KT, Akoya Biosciences, USA). Briefly, a 4-μm-thick section was cut from formalin-fixed paraffin-embedded kidney tissues for each panel detection. The slides were deparaffinized, rehydrated, and subjected to epitope retrieval by boiling in citrate buffer (pH 6) for 20 min at 97 °C. Endogenous peroxidase was then blocked by incubation in 3% H_2O_2 for 15 min, and tissue sections were covered with blocking buffer for 10 min at room temperature. Only one antigen was detected in each round, including primary antibody incubation, secondary antibody incubation, and tyramine signal amplification (TSA) visualization, followed by labeling the next antibody after epitope retrieval and protein blocking as before. KIM1 (1:100, AF1817, R&D, USA), PCNA (1:1000, ab92552, Abcam, UK), and endomucin (1:200, sc-65495, Santa Cruz, CA, USA) were sequentially detected. The slides were scanned using a PerkinElmer Vectra (Vectra 3.0.5; PerkinElmer, USA).

Immunofluorescence staining

Immunofluorescence staining was performed as described previously [30]. The primary antibodies used were as follows: α-SMA (1:200, ab7817, Abcam, UK) and fibronectin (1:200, ab2413, Abcam, UK). The stained slides were scanned with a high-content imaging system (Operetta CLS, Perkin Elmer, USA).

Quantitative real-time PCR (qRT–PCR)

Total RNA was isolated with TRIzol reagent (Invitrogen, Carlsbad, CA, USA) according to the manufacturer's instructions. The mRNA levels were determined by qRT–PCR analysis with an Applied Biosystems 7500 system (Applied Biosystems, Foster City, CA, USA). The list of primers is presented in Supplementary Table 1.

Enzyme-linked immunosorbent assay (ELISA)

Blood was obtained from the inferior vena cava and centrifuged for 15 min at 3000 rpm to separate the serum. Mouse VEGF ELISA Kits (EK283/2, Multi-Science, China) were used to detect the serum VEGF levels according to the manufacturer's instructions.

Liquid chromatography–mass spectrometry (LC–MS/MS) proteomics analysis

LC–MS/MS analysis was performed according to a previously described method [31]. MS/MS spectra were searched using Proteome Discoverer (version 2.2, Thermo Fisher Scientific, USA) against the UniProt proteome database (UniProt_Mouse_84433_20180102.fasta), and the label-free quantitation algorithm was used for quantitative analysis. Quantifiable proteins were defined as those identified at least twice in the three biological replicates. The criteria for a statistically significant difference in protein expression were a fold change in abundance >1.2 and an adjusted P value <0.05.

Statistical analysis

Statistical analysis was performed using GraphPad Prism software. All data are expressed as the means ± standard deviations (SDs). For continuous variables, significant differences were determined by 2-tailed unpaired Student's t test for comparisons between 2 groups or 1-way ANOVA with a post hoc test for comparisons among more than 2 groups. A value of $P < 0.05$ was considered to indicate significance.

Study approval

All animals were handled in strict accordance with the procedures that were reviewed and approved by the Institutional Animal Care and Use Committee of the Chinese PLA General Hospital.

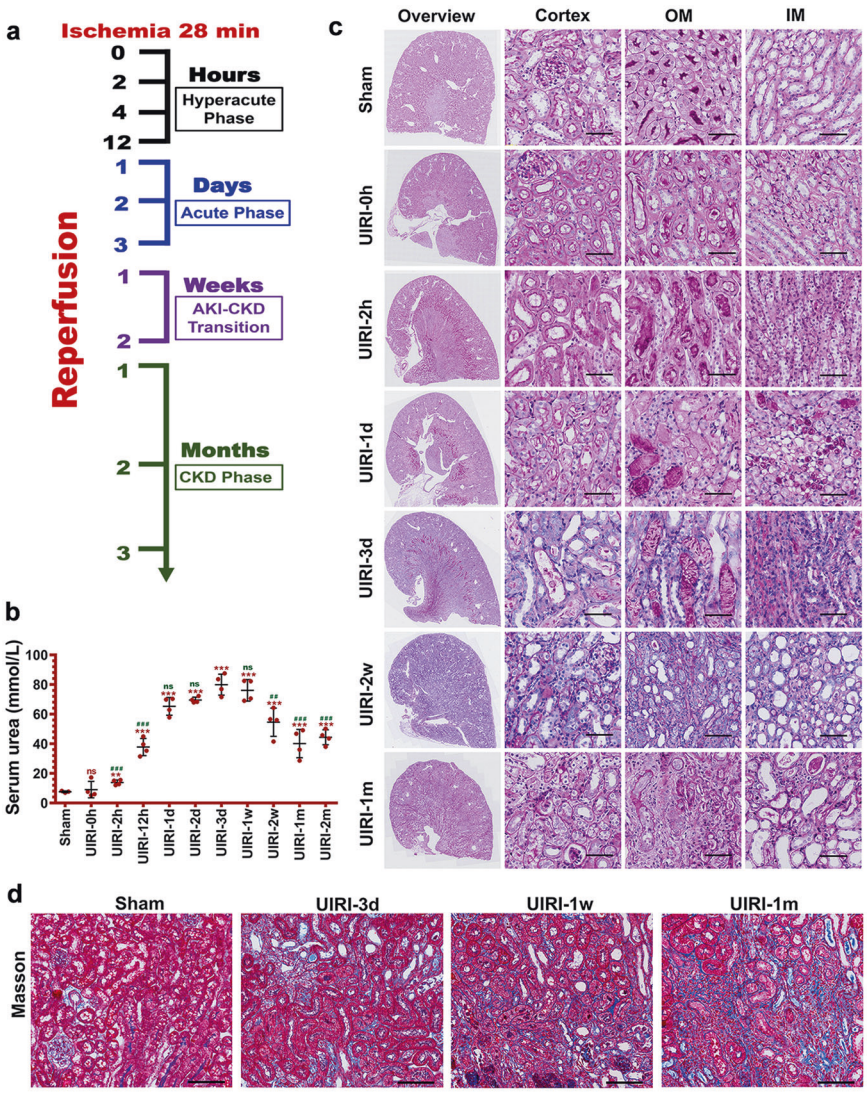

Fig. 1 Incomplete recovery after 28 min of renal unilateral IRI. a Experimental design and sample collection time points. **b** Serum urea of sham and UIRI mice with different reperfusion time. **c** Representative PAS staining of the sham and UIRI kidneys at different time. Scale bar 50 μm. **d** Representative micrographs showing Masson staining of renal collagen deposition at 3 days, 1 week, and 4 weeks after UIRI. Scale bar 100 μm. Data are shown as mean ± SD. Statistical analyses were performed using 1-way ANOVA with a post hoc test (**b**). $n = 4$. $^{***}P < 0.001$ vs. sham; $^{\#\#}P < 0.01$, $^{\#\#\#}P < 0.001$ vs. UIRI 3d. ns no significance, OM Outer Medulla, IM Inner Medulla.

RESULTS

Characterization of renal pathology in a progressive AKI mouse model

To determine the landscape of AKI pathology from initial injury to fibrosis progression, we examined mice with AKI at 13 different time points after UIRI: the hyperacute phase (2, 4, and 12 h), the acute phase (1, 2, and 3 days), the AKI-CKD transition phase (1 and 2 weeks), and the CKD phase (1, 2 and 3 months) (Fig. 1a). As expected, the serum urea levels were markedly elevated 2 h after UIRI, peaked on day 3 and gradually returned to baseline at 1 week postischemia (Fig. 1b). Representative PAS staining from different AKI phases is shown in Fig. 1c. As shown, tubular injury in the outer medullary region could be observed as early as 2 h after UIRI, and the injury was most severe in the cortical medullary junction area on day 1. Focal atrophic tubules began to appear as the kidneys transitioned to CKD one week after UIRI. At 1 month, CKD developed, and areas of tubular atrophy, interstitial fibrosis, and chronic inflammation were observed. Masson's staining, as shown in Fig. 1d, revealed that fibrosis was restricted to the outer medullary region adjacent to damaged S3 segments on day 3 and was deposited in both inner and outer medullary regions at 1 week. By 1 month after UIRI, massive collagen fiber deposition could be observed throughout the kidneys.

Comprehensive expression and localization of extraglomerular VEGFA during the progression of AKI to renal fibrosis

To obtain an initial overview of the expression of proangiogenic and antiangiogenic factors in various AKI phases, we searched the Gene Expression Omnibus (GEO) database and downloaded the gene expression profile GSE98622 [32], which contained a detailed molecular characterization of gene expression in a murine model of IRI at the 12-month timepoint. The heatmap in Fig. 2a shows the angiogenesis-related genes, and among these, *Vegfa* was the most significantly upregulated gene 2–4 h after injury. As shown in Fig. 2b, c, the renal VEGFA mRNA and protein expression levels were increased in the injured mice as early as 2 h and only decreased to levels below those observed in the sham-operated control mice. The inhibition of VEGFA expression continued up to 3 days postischemia and gradually increased again in the AKI-CKD transition period. Thus, two peaks of renal VEGFA expression were

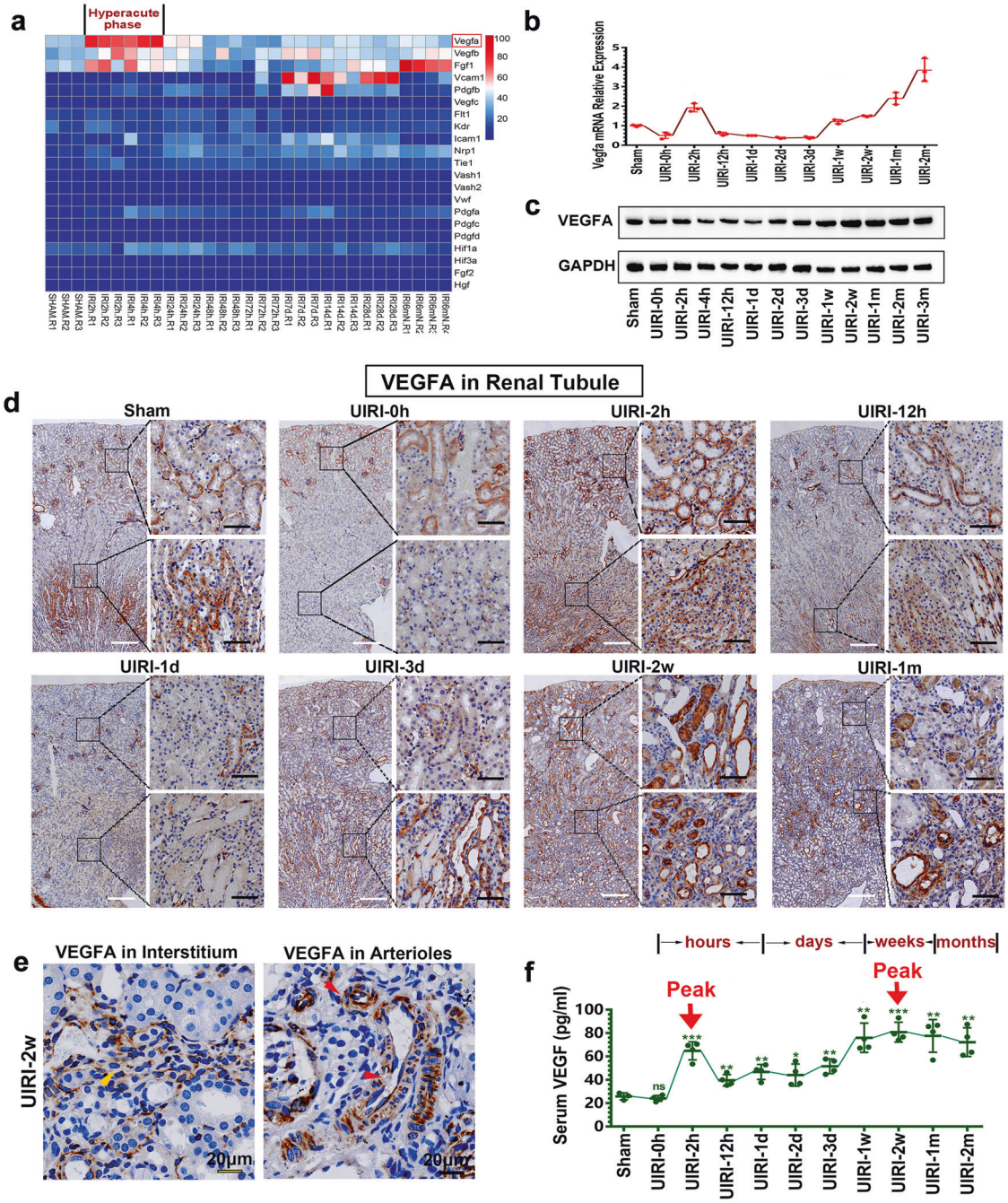

Fig. 2 Comprehensive expression and localization of extraglomerular VEGFA in the progressive AKI. a Heatmap of RNA-seq data showing the expression of angiogenesis-related genes in gene expression profile GSE98622, which contained a detailed molecular characterization of a murine IRI model for 12 months. **b**, **c** Vegfa mRNA and protein expression in mouse kidney tissues at different time points after UIRI. **d** Immunohistochemical analysis of VEGFA expression in renal tubules was performed at different time points after UIRI. White scale bars: 250 μm. Black scale bars: 50 μm. **e** Immunohistochemical analysis of VEGFA expression in renal interstitium (yellow arrow) and arterioles (red arrow) at 2 weeks after AKI. Scale bars: 20 μm. **f** Serum levels of VEGF at different time points after UIRI. Data are shown as mean ± SD. Statistical analyses were performed using 1-way ANOVA with a post hoc test. $n = 4$. $^{*}P < 0.05$, $^{**}P < 0.01$, $^{***}P < 0.001$ vs. sham. ns no significance.

detected during the progression of AKI: one occurred in the hyperacute phase, and the other occurred in the AKI-CKD transition phase. To determine the extraglomerular localization of VEGFA, immunohistochemical staining was performed. The tubular expression of VEGFA was localized to the thick ascending limb and the proximal and distal cortical tubules (Fig. 2d). During the first 2 h after UIRI, VEGFA in the proximal tubule was secreted and released into the peritubular capillaries through the tubular basement membrane (Supplementary Fig. 1). Interestingly, during the AKI-CKD transition and CKD phases, increased renal VEGFA protein expression was observed not only in the tubules but also in the interstitial cells (Fig. 2e). To further identify the interstitial cells in which VEGFA was expressed, single-cell analysis was performed using a publicly available dataset from an AKI murine model at the 3-day time point (https://ngdc.cncb.ac.cn/gsa/browse/CRA006298) [33], and immunofluorescence was conducted to costain VEGFA with markers of

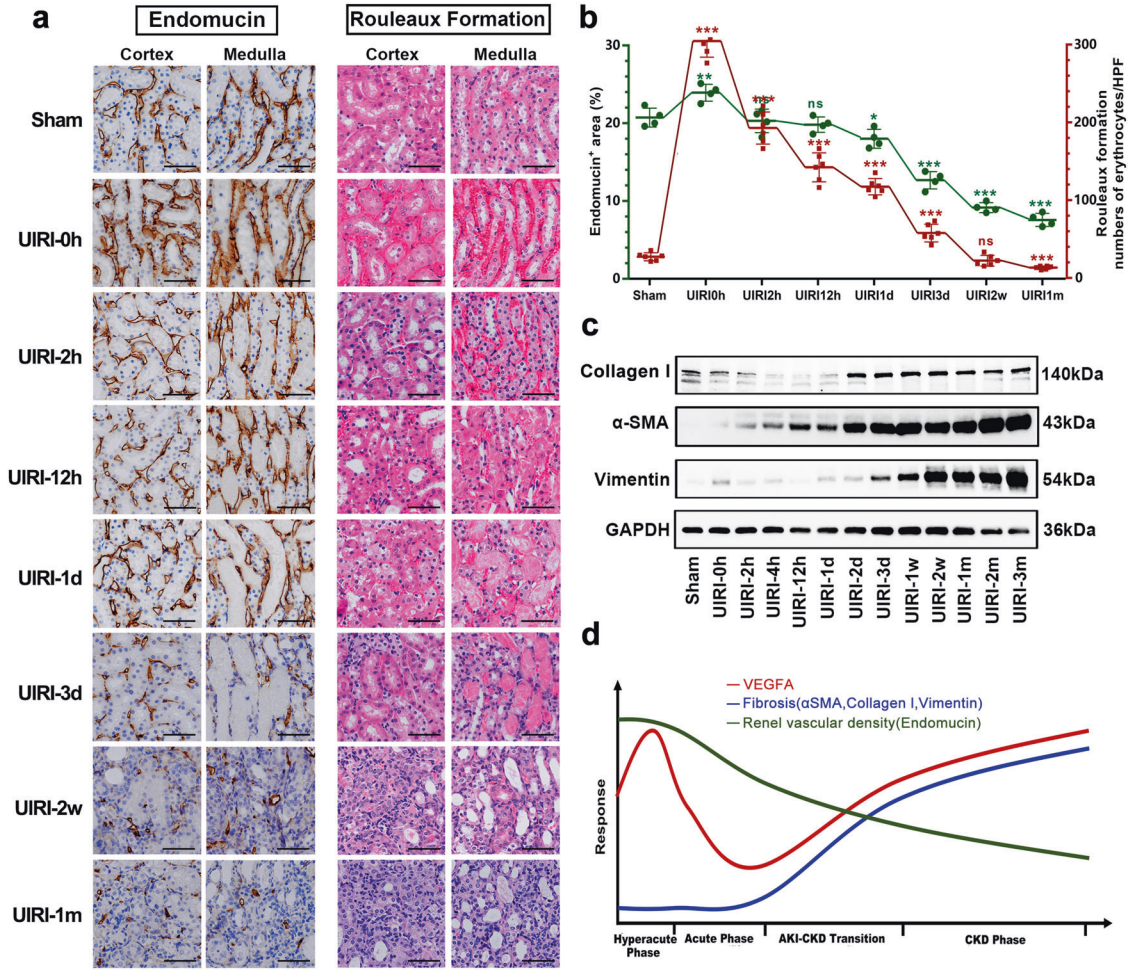

Fig. 3 Correlation analysis of microvascular density, VEGFA expression, and renal fibrosis in the AKI process. a Representative immunohistochemical staining of Endomucin and HE staining of rouleaux formation in renal cortical and medullary sections at different time points after UIRI. Scale bars: 50 μm. **b** Quantitative analysis of the Endomucin-positive areas (green) and quantification of rouleaux formation (red). **c** Western blot of fibrosis markers (collagen I, α-SMA, vimentin) in injured kidneys at different times after UIRI. **d** Correlation of microvascular density, VEGFA, and renal fibrosis in the AKI process. Data are shown as mean ± SD. Statistical analyses were performed using 1-way ANOVA with a post hoc test. $n = 4$. *$P < 0.05$, **$P < 0.01$, ***$P < 0.001$ vs. sham. ns no significance.

renal interstitial cells to clarify the expression and localization of VEGFA during AKI progression. These results confirmed that VEGFA was also expressed in fibroblasts/myofibroblasts and macrophages (Supplementary Figs. 2–4). In addition to exploring the expression of VEGFA in the kidneys, we also measured the changes in the serum levels of VEGF at different periods of AKI (Fig. 2f). The level of serum VEGF increased instantaneously in the 2 h immediately after AKI and then decreased gradually. The level then increased again in the period of AKI-CKD transition, which was consistent with the change in VEGFA expression observed in the kidney.

Correlation analysis of the microvascular density, VEGFA, and renal fibrosis in the AKI process

The peritubular microvascular density, as assessed by the endothelial marker endomucin, was slightly reduced in the early injury phase. However, with the progression of AKI, the peritubular capillary lumen becomes narrowed or even occluded. A significant and sustained vascular dropout was observed on day 3, and a nearly 50% decrease in the vascular density was detected 4 weeks after ischemic insult (Fig. 3a, b). These data suggest that, unlike renal epithelial tubular cells, the renal vascular system lacks comparable regenerative potential. Additionally, there was marked microvascular plugging mediated by rouleaux formation, and adhesion was observed after 28 min of ischemia but no reperfusion. The microvascular plugging was slightly attenuated but remained at high levels from 2 h to 1 day of reperfusion, leading to reduced flow and worsening ischemia. A significant reduction in rouleaux formation was observed beginning on day 3, which was possibly due to marked vascular dropout (Fig. 3a, b). We also performed a correlation analysis of VEGFA expression, microvascular density, and renal fibrosis throughout the AKI process (Fig. 3c, d). With the gradual increase in VEGFA expression during the AKI-CKD transition and CKD phases, renal fibrosis (as assessed by collagen I, α-SMA, and vimentin) was aggravated, whereas the decrease in peritubular capillary density was consistent with the degree of interstitial fibrosis. It seems that capillary rarefaction persists and progresses despite high expression of VEGFA in CKD.

Early exogenous VEGFA therapy protects against AKI by preserving the renal microvessel structure and counteracting secondary hypoxic insults

To investigate the hypothesis that early VEGFA supplementation protects against AKI, we intravenously administered VEGFA protein to mice beginning at the time of reperfusion, and the mice were sacrificed on day 3 (Fig. 4a). As shown in Fig. 4b, the serum creatinine (Scr) levels were increased significantly in the vehicle-treated UIRI mice compared with the sham mice. Notably,

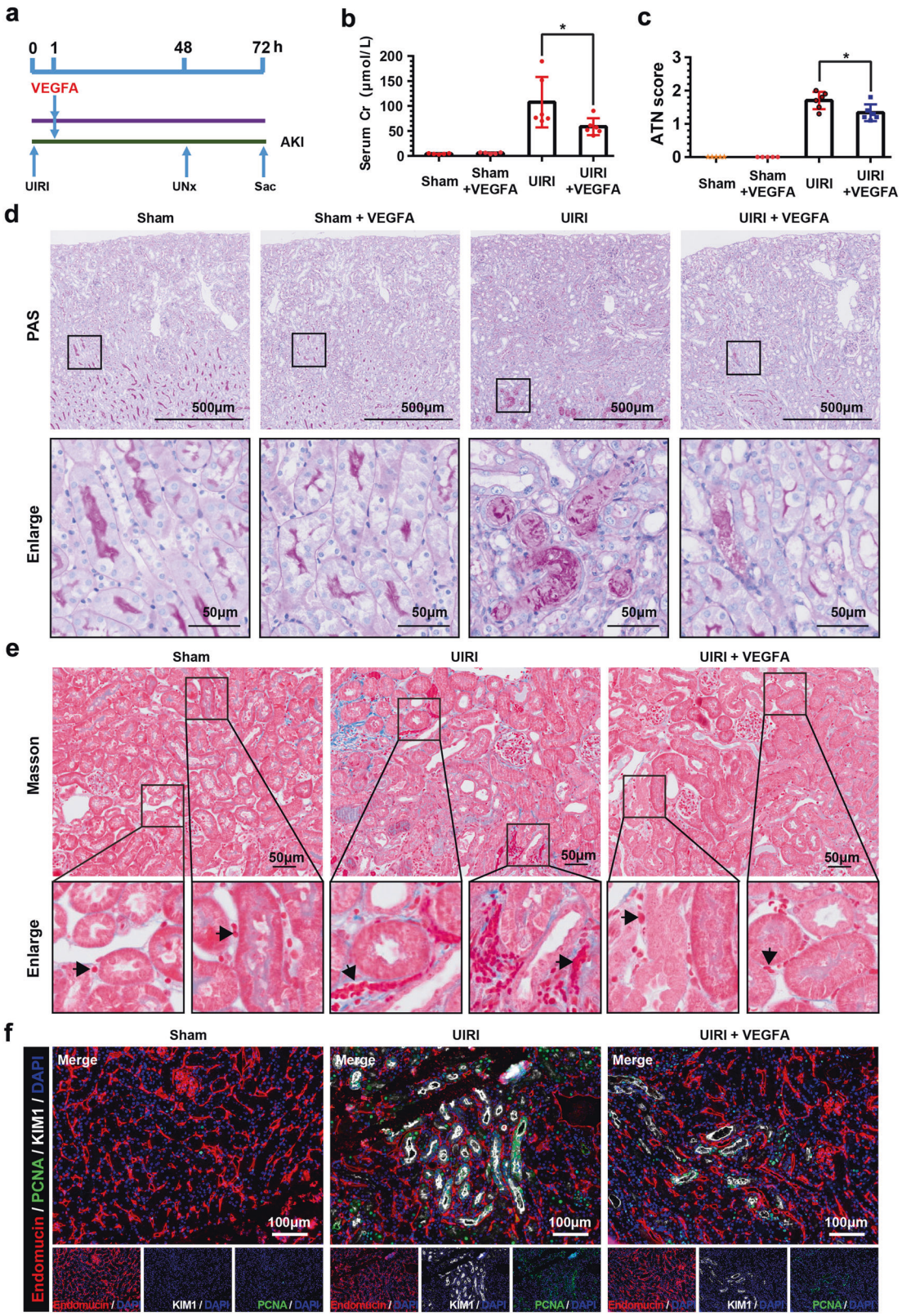

Fig. 4 Early exogenous VEGFA therapy protects against AKI by preserving renal microvessel structure and counteracting secondary hypoxic insults. a Experimental design. **b** Serum creatinine levels in the groups at 3 days after UIRI. $n = 5$-6 mice per group. **c** Quantitative assessment of tubular damage. $n = 10$ fields per mice. **d** Representative micrographs of PAS staining showing kidney injury in UIRI mice after early exogenous VEGFA therapy. **e** Representative micrographs of rouleaux formation in Masson–stained kidney sections in the groups after UIRI. **f** Representative multiplex fluorescent IHC staining showing the presence of endomucin (red color, marker of microvascular density), KIM1 (white color, marker of injured tubules), PCNA (green color, marker of proliferating cells) in UIRI mice after early exogenous VEGFA therapy. Data are shown as mean ± SD. Statistical analyses were performed using 1-way ANOVA with a post hoc test (**b** and **c**). *$P < 0.05$ vs. sham.

the Scr levels were decreased in the early VEGFA therapy group compared with the vehicle-treated UIRI group (Fig. 4b). PAS staining and ATN scores revealed less tubular injury in the VEGFA group than in the UIRI group (Fig. 4c, d). Rouleaux formation, which is a marker of microvascular congestion, tended to be attenuated in the VEGFA group (Fig. 4e). We further verified the microvascular density, tubular injury, and cell proliferation by measuring endomucin, KIM1, and PCNA expression using the multiplex fluorescent IHC method. The early VEGFA-treated mice had smaller percentages of injured tubules (KIM1) than the vehicle-treated mice with UIRI (Fig. 4f).

Late anti-VEGFA treatment attenuates renal fibrosis progression

To investigate the therapeutic effect of late anti-VEGFA treatment, we administered VEGFA-neutralizing antibody to mice on day 7 after UIRI and sacrificed them on day 14 (Fig. 5a). A significant decrease in the Scr level was observed in the late anti-VEGFA-treated group relative to the vehicle-treated group (Fig. 5b). On day 14, focal atrophic tubules, interstitial fibrosis and chronic inflammation began to appear in the vehicle-treated UIRI group as the kidneys transitioned to CKD, whereas late anti-VEGFA treatment alleviated tubular atrophy and chronic inflammation (Fig. 5c). ECM accumulation (collagen deposition) was initially assessed by Masson's staining. Fewer fibrotic areas were observed in the anti-VEGFA group than in the vehicle-treated groups (Fig. 5d). Fibronectin/α-SMA costaining and Western blotting analysis of α-SMA/collagen I expression were carried out to confirm the antifibrotic effects of anti-VEGFA (Fig. 5e, f).

Proteomic analysis of the molecular mechanism through which anti-VEGFA alleviates renal fibrosis

To elucidate the molecular mechanism through which anti-VEGFA attenuates renal fibrosis progression, a mass spectrometric analysis of mouse kidneys was performed using label-free technology. We performed a principal component analysis (PCA) of those samples (different colors) to visualize sample clusters. The results showed that samples in the groups were clustered (Fig. 6a). A total of 792 proteins were downregulated in the sham versus 14-d UIRI group, whereas a total of 394 proteins were downregulated in the anti-VEGFA + 14-d UIRI versus 14-d UIRI group. A total of 336 proteins were commonly downregulated in both compared groups (Fig. 6b). A Kyoto Encyclopedia of Gene and Genomes (KEGG) enrichment analysis of commonly downregulated proteins revealed that several signaling pathways, including leukocyte transendothelial migration, focal adhesion, platelet activation, adherens junctions, and tight junctions, were enriched (Fig. 6c). A biological process description of Gene Ontology (GO) terms further illustrated that 79 of the 336 commonly downregulated proteins were involved in interstitial fibrotic events (such as regulation of supramolecular fiber organization, cell-matrix adhesion, myofibril assembly, fibroblast migration, stress fiber assembly, and epithelial cell migration) (Fig. 6d), which could be attributed to the therapeutic alleviation of renal fibrosis by anti-VEGFA. By searching the STRING database (http://string-db.org/), all 79 fibrosis-related proteins with decreased expression met the criterion of a combined score >0.4. Fifteen hub proteins were further mined by the cyto-Hubba plugin in Cytoscape software (Fig. 6e) and were validated by PCR. Detailed information on the 15 hub proteins is listed in Supplementary Table 2 and Supplementary Fig. 5.

DISCUSSION

Despite recent dramatic progress in the knowledge of the role of VEGFA in progressive renal disease, the expression and molecular characterization of this mitogen in the kidney under different conditions and at different time points remain unclear. In this research, we characterized the landscape of VEGFA expression in mouse kidneys with the aims of elucidating the exact spatiotemporal role of extraglomerular VEGFA during the progression of initial AKI to renal fibrosis and proposing more effective treatment strategies based on the understanding of these mechanisms (Fig. 7).

At the initial phase after hypoxic insults, the VEGFA levels rapidly increased and peaked within 2 h of reperfusion, which is consistent with the results of a pilot study of 29 patients during cardiac surgery [34]. The early high expression of VEGFA, stimulated by hypoxia-inducible factor and some other immediate early transcription factors, may represent an adaptive mechanism that protects against AKI at the hyperacute phase [35]. However, despite persistent hypoxia, VEGFA expression is downregulated 1–3 days after AKI, possibly because injured tubular cells are not able to express a sufficient amount of VEGFA. During the AKI-CKD transition phase, the level of renal VEGFA was significantly upregulated again and gradually reached a second peak. The high expression of VEGFA might be partly due to repaired tubular epithelial cells, which resynthesize and secrete VEGFA under hypoxic conditions. In addition, as shown by our experiments and single-cell sequencing results, a large number of renal interstitial cells could also express VEGFA. This finding may be the main reason for the high expression of VEGFA during CKD. Because the change in the serum VEGF levels is consistent with that in the kidney, the circulating VEGF levels may be used as a biomarker for monitoring AKI-to-CKD progression. Moreover, differences in the expression levels and renal location of VEGFA at the early AKI and late CKD phases suggest that VEGFA may play complex roles in the kidney depending on certain conditions and time points.

However, although renal VEGFA was highly expressed during the AKI-CKD transition phase, peritubular microvascular density was still significantly reduced, and VEGFA expression was positively correlated with the degree of interstitial fibrosis. These contradictory and perplexing findings led us to reconsider the following: *(1) Why does capillary rarefaction persist and progress despite VEGFA expression in CKD?* Although the proangiogenic factor VEGFA is abundantly expressed during the AKI-CKD transition, other antiangiogenic substances, such as thrombospondin-1, endostatin, and ADAMTS-1, are also upregulated during this stage [14, 36, 37]. Disruption of the balance of local angioregulatory factors may be one contributor to microvascular rarefaction. In addition, in contrast to proximal tubules, the renal vasculature lacks comparable regenerative potential. Direct injury or death to endothelial cells by hypoxic insults and low proliferative capacity led to a persistent 50% reduction in the vascular density after UIRI in our study, which is consistent with previous studies [38]. Moreover, endothelial-to-mesenchymal transition is a common phenomenon that compromises vascular integrity during the pathogenesis of fibrosis [39, 40]. All these factors are thought to be key contributors that lead to persistent microvascular rarefaction despite high expression of VEGFA in CKD. *(2) What is the role of VEGFA in progressive renal disease? Does VEGFA participate in interstitial fibrosis?* As confirmed by other studies, VEGFA overexpression increases fibroblast proliferation, myofibroblast activation, and collagen content in multiple organs, including the liver, heart, skin, and lungs, during fibrosis development [18–21]. Higher VEGF concentrations also predict adverse renal progression in patients with diabetic chronic kidney disease [41]. The profibrotic effects of VEGFA are likely mediated by both proinflammatory and noninflammatory mechanisms. VEGFA induces proinflammatory chemotactic cytokines, including IL-8, MCP-1, TNFα, and MIP-1 [21], contributing to the recruitment of monocytes/macrophages into the interstitium [42]. In addition, VEGFA can shift M0 macrophages to the M2 phenotype [43], which promotes renal fibrosis via paracrine effects or direct transition to myofibroblast-like cells. The increased macrophages/fibroblasts further secrete more VEGFA, which leads to a vicious cycle accelerating fibrosis. In addition, there is another viewpoint that VEGFA may directly induce collagen synthesis in fibroblasts via interaction with platelet-derived growth factor receptors (PDGFRs) rather than VEGFRs [21]. However, this finding has only

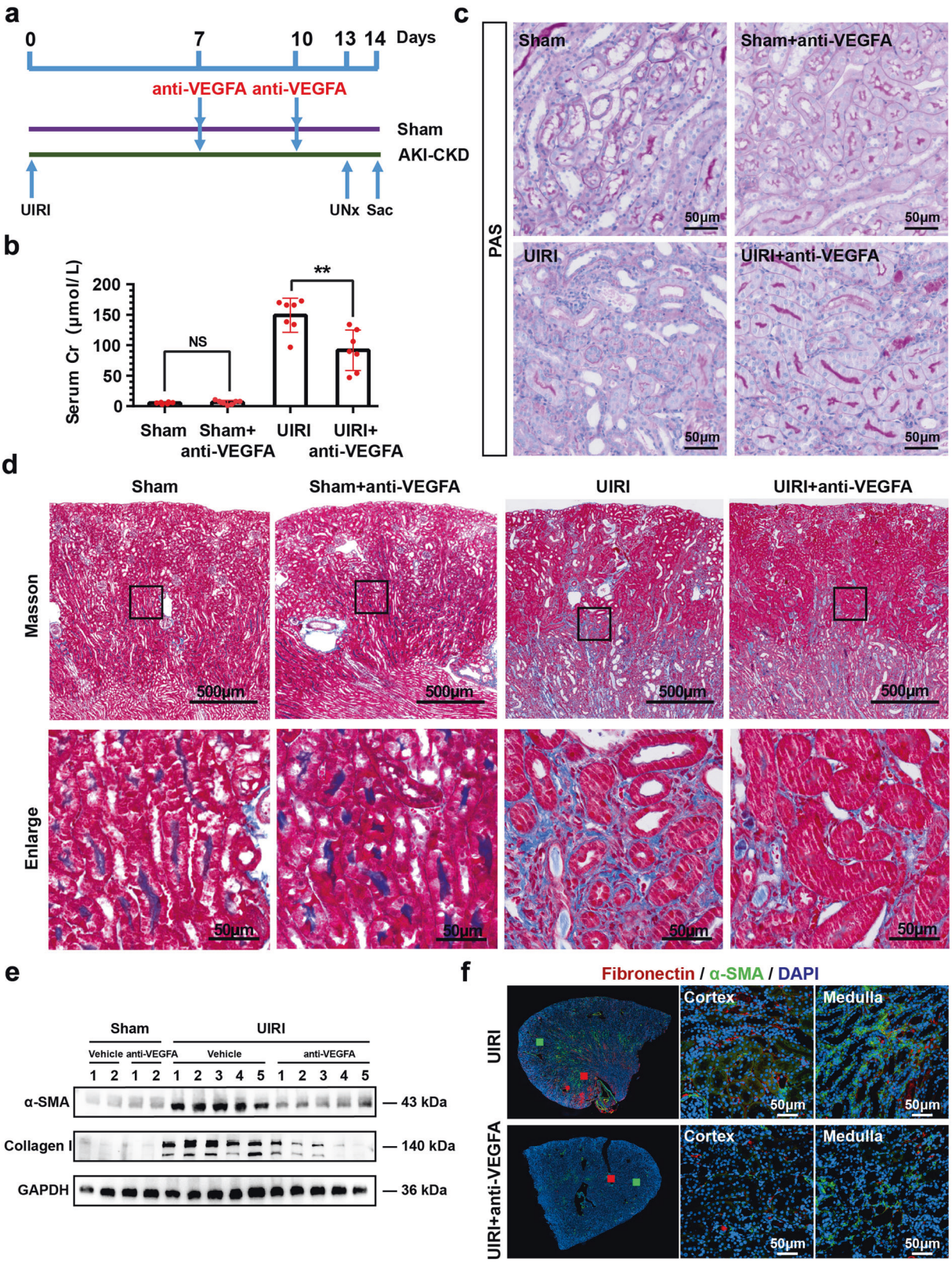

Fig. 5 Late anti-VEGFA treatment attenuates renal fibrosis progression. a Experimental design. **b** Serum creatinine levels in the groups. **c** Representative micrographs showing PAS staining in the various groups. **d** Representative micrographs showing Masson staining of renal collagen deposition at 14 days after UIRI in the various groups as indicated. **e** Western blot analysis of α-SMA and collagen I in injured kidneys in the various groups as indicated. **f** Representative immunofluorescence staining of α-SMA (green) and fibronectin (red) in the groups after 14 days of UIRI. Scale bars: 50 μm. $n = 5–7$ mice per group.

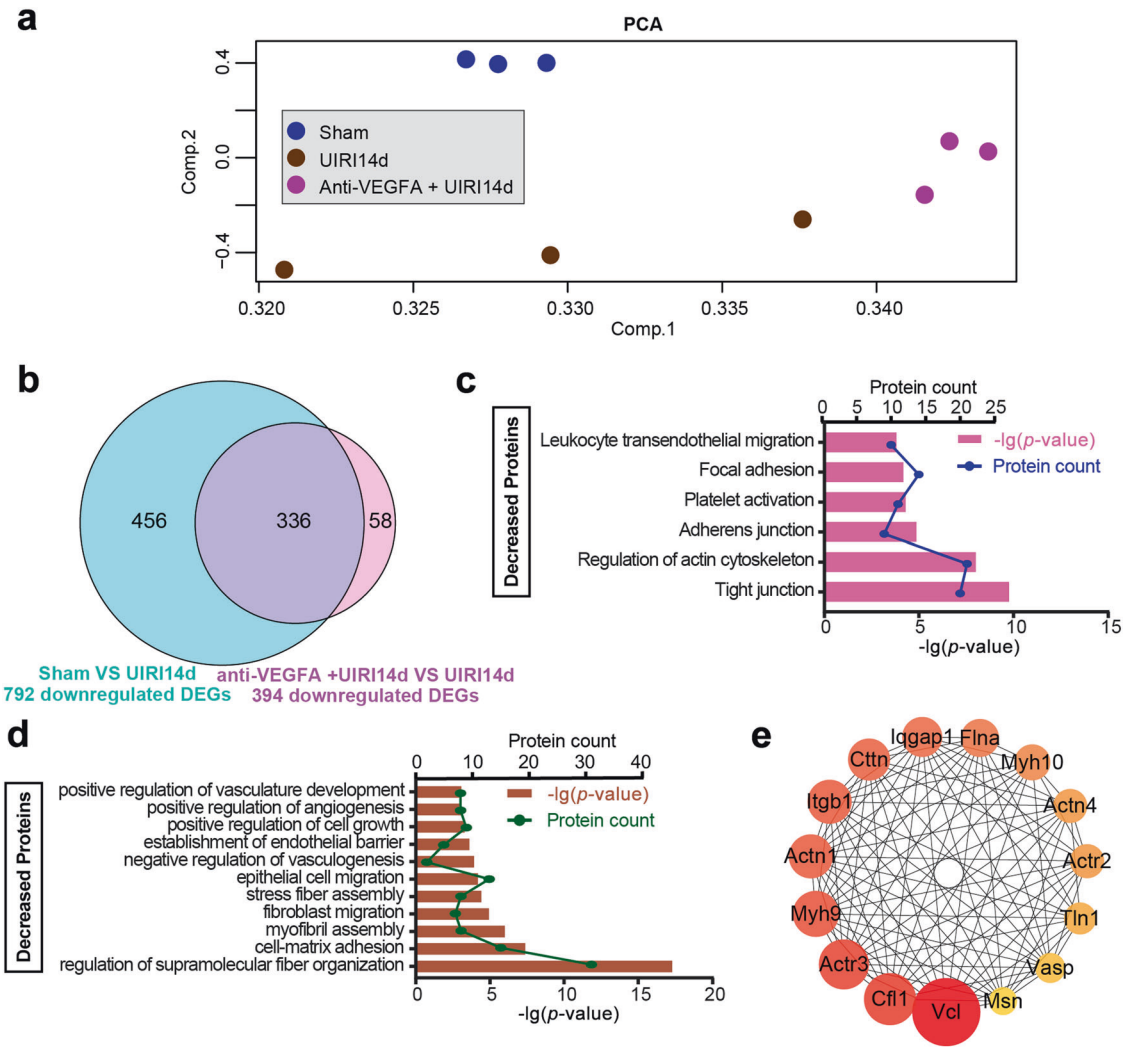

Fig. 6 Proteomic analysis for the molecular mechanism of renal fibrosis alleviation by anti-VEGFA. a Principle component analysis (PCA) plot of different groups. **b** Identification of overlapping downregulated proteins in Sham versus UIRI 14d groups and anti-VEGFA + UIRI 14d versus UIRI 14d groups. **c**, **d** KEGG pathway and GO biologic process analysis involved in interstitial fibrotic events of decreased proteins were plotted with protein count and significance (*P* value). **e** The protein-protein interaction (PPI) network of the 15 down-regulated hub proteins was visualized with Cytoscape.

been verified in skin fibroblasts of systemic sclerosis. Due to the heterogeneity of fibroblasts, whether this viewpoint is applicable to the kidney remains to be further confirmed.

This better understanding of these mechanisms at the early AKI and late CKD phases offers important opportunities for us to design intervention strategies that target VEGFA differently depending on the duration of its expression. In our study, we confirmed that early VEGFA supplementation after AKI exerts a renoprotective effect. Endothelial injury of peritubular capillaries and the deficiency of VEGFA in the setting of acute injury result in reductions in the postischemic blood flow and microvascular density, as well as increases in microvascular plugging and coagulation. This cascade of events, in turn, accelerates hypoxic and inflammatory injury in the renal parenchyma. Thus, early exogenous supplementation of VEGFA can help prevent endothelial cell apoptosis and improve the regenerative capacity of endothelial cells, which is necessary for repairing the microvessel structure. VEGFA can also improve the renal microcirculation by activating eNOS and increasing the ratio of p-eNOS to total eNOS, counteracting secondary hypoxic insults [16]. The other potential mechanism of early renal protection with VEGFA also includes promotion of the mobilization and recruitment of endothelial progenitor cells (EPCs) to protect the kidneys [44]. These results are consistent with increasing evidence that highlights the importance of VEGFA at the early stages of AKI [15, 16, 45]. A large prospective cohort study of adults undergoing cardiac surgery reported that higher postoperative VEGF levels within 6 h after surgery are associated with lower AKI and mortality risks [46], which further confirms the importance of early VEGFA intervention for AKI protection. Because high VEGFA expression promotes fibrotic progression at the CKD phase, we attempted to treat renal fibrosis with a VEGFA-neutralizing antibody, which has been proven to be an effective therapeutic strategy. We further explored the potential mechanisms of renal fibrosis alleviation by anti-VEGFA. A proteomic analysis showed that anti-VEGFA may attenuate renal fibrosis by directly or indirectly affecting the supramolecular fiber organization, cell-matrix adhesion, fibroblast migration, vasculogenesis, and other factors.

Although anti-VEGFA offers benefits in the traditional treatment of both solid tumors and renal fibrosis, as revealed by our findings, its use is reportedly associated with nephrotoxicity. Podocyte injury is one of the most common nephrotoxic injuries associated with pharmacological VEGF inhibition [47]. However, we did not observe additional kidney damage with anti-VEGFA therapy, possibly

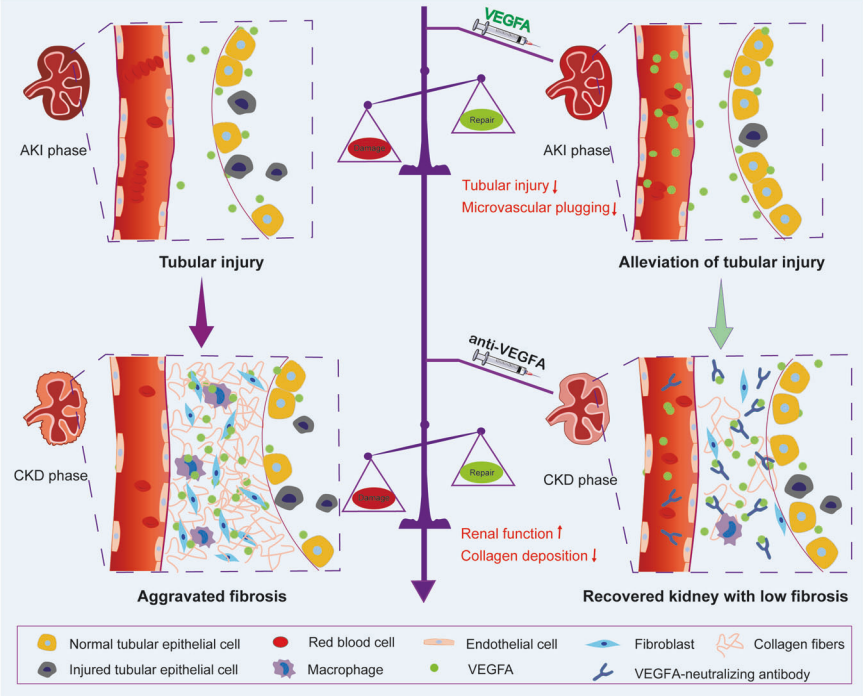

Fig. 7 Schematic illustration depicting the dual role of VEGFA in regulating early acute kidney injury and late fibrosis. Early VEGFA supplementation protected against renal injury by preserving microvessel structures and counteracting secondary tubular hypoxic insults, whereas late anti-VEGFA treatment attenuated renal fibrosis progression.

because VEGFA-neutralizing antibody was used only for a short period of time in our research and had not yet caused damage.

Our study demonstrates that renal VEGFA expression increases during both the hyperacute injury phase and the AKI-CKD transition period. VEGFA plays dual roles in regulating early injury and late fibrosis. Exogenous VEGFA therapy protects against early tubular injury, whereas inhibition of VEGFA at the late stage attenuates renal fibrosis.

DATA AVAILABILITY

The data underlying this article will be shared on reasonable request to the corresponding author.

ACKNOWLEDGEMENTS

This work was supported by Beijing Natural Science Foundation (7222169); National Natural Science Foundation of China (82000631, 82070741, 82030025, 82100713 and 32200579); Young Elite Scientist Sponsorship Program by CAST (YESS20200400); National Key Research and Development Project (2018YFE0126600); Young Talent Project of Chinese PLA General Hospital (20230404).

AUTHOR CONTRIBUTIONS

MJH: experiments design, collection and assembly of data, data analysis and interpretation, and manuscript writing. YWJ: animal surgery, collection and assembly of data, data analysis and interpretation. JWC and LLW: data analysis and interpretation. DL, TZ, XFL, YFZ, and XY: conducting experiments. PQ and XW: performing all bioinformatics associated with this study. XFS, GYC and XMC: experiments design. ZF and QH: financial support, conception and design, manuscript revision, final approval of manuscript.

ADDITIONAL INFORMATION

Supplementary information The online version contains supplementary material available at https://doi.org/10.1038/s41401-023-01070-1.

Competing interests: The authors declare no competing interests.

REFERENCES

1. Bellomo R, Kellum JA, Ronco C. Acute kidney injury. Lancet. 2012;380:756–66.
2. Venkatachalam MA, Weinberg JM, Kriz W, Bidani AK. Failed tubule recovery, AKI-CKD transition, and kidney disease progression. J Am Soc Nephrol. 2015;26:1765–76.
3. Kovesdy CP. Epidemiology of chronic kidney disease: an update 2022. Kidney Int Suppl. 2022;12:7–11.
4. Mantovani A, Zusi C. PNPLA3 gene and kidney disease. Exploration Med. 2020;1:42–50.
5. Rashid I, Katravath P, Tiwari P, D'Cruz S, Jaswal S, Sahu G. Hyperuricemia—a serious complication among patients with chronic kidney disease: a systematic review and meta-analysis. Exploration Med. 2022;3:249–59.
6. Humphreys BD. Mechanisms of renal fibrosis. Annu Rev Physiol. 2018;80:309–26.
7. Tanabe K, Wada J, Sato Y. Targeting angiogenesis and lymphangiogenesis in kidney disease. Nat Rev Nephrol. 2020;16:289–303.
8. Tanaka S, Tanaka T, Nangaku M. Hypoxia and dysregulated angiogenesis in kidney disease. Kidney Dis. 2015;1:80–9.
9. Mao H, Jiang C, Xu L, Chen D, Liu H, Xu Y, et al. Ginsenoside protects against AKI via activation of HIF-1α and VEGF-A in the kidney-brain axis. Int J Mol Med. 2020;45:939–46.
10. Liu F, Lou YL, Wu J, Ruan QF, Xie A, Guo F, et al. Upregulation of microRNA-210 regulates renal angiogenesis mediated by activation of VEGF signaling pathway under ischemia/perfusion injury in vivo and in vitro. Kidney Blood Press Res. 2012;35:182–91.
11. Villanueva S, Cespedes C, Gonzalez A, Vio CP. bFGF induces an earlier expression of nephrogenic proteins after ischemic acute renal failure. Am J Physiol Regul Integr Comp Physiol. 2006;291:R1677–87.
12. Qin LL, Xue F, Yin F, Zhao J, Zhang KY. Expression of syndecan-1, PKC and VEGF in rats with acute kidney injury and correlation between syndecan-1 and renal function. Eur Rev Med Pharmacol Sci. 2020;24:12794–801.
13. Sánchez-Navarro A, Pérez-Villalva R, Murillo-de-Ozores AR, Martínez-Rojas M, Rodríguez-Aguilera JR, González N, et al. Vegfa promoter gene hypermethylation at HIF1α binding site is an early contributor to CKD progression after renal ischemia. Sci Rep. 2021;11:8769.
14. Basile DP, Fredrich K, Chelladurai B, Leonard EC, Parrish AR. Renal ischemia reperfusion inhibits VEGF expression and induces ADAMTS-1, a novel VEGF inhibitor. Am J Physiol Ren Physiol. 2008;294:F928–36.
15. Tögel F, Zhang P, Hu Z, Westenfelder C. VEGF is a mediator of the renoprotective effects of multipotent marrow stromal cells in acute kidney injury. J Cell Mol Med. 2009;13:2109–14.

16. Bai Y, Zhang Y, Yang S, Wu M, Fang Y, Feng J, et al. Protective effect of vascular endothelial growth factor against cardiopulmonary bypass-associated acute kidney injury in beagles. Exp Ther Med. 2018;15:963–9.
17. Xu Y, Jiang W, Zhong L, Li H, Bai L, Chen X, et al. miR-195-5p alleviates acute kidney injury through repression of inflammation and oxidative stress by targeting vascular endothelial growth factor A. Aging. 2020;12:10235–45.
18. Sahin H, Borkham-Kamphorst E, Kuppe C, Zaldivar MM, Grouls C, Al-samman M, et al. Chemokine Cxcl9 attenuates liver fibrosis-associated angiogenesis in mice. Hepatology. 2012;55:1610–9.
19. Zhao H, Bian H, Bu X, Zhang S, Zhang P, Yu J, et al. Targeting of discoidin domain receptor 2 (DDR2) prevents myofibroblast activation and neovessel formation during pulmonary fibrosis. Mol Ther. 2016;24:1734–44.
20. Barratt SL, Blythe T, Ourradi K, Jarrett C, Welsh GI, Bates DO, et al. Effects of hypoxia and hyperoxia on the differential expression of VEGF-A isoforms and receptors in Idiopathic Pulmonary Fibrosis (IPF). Respir Res. 2018;19:9.
21. Maurer B, Distler A, Suliman YA, Gay RE, Michel BA, Gay S, et al. Vascular endothelial growth factor aggravates fibrosis and vasculopathy in experimental models of systemic sclerosis. Ann Rheum Dis. 2014;73:1880–7.
22. Lin Y, Dong MQ, Liu ZM, Xu M, Huang ZH, Liu HJ, et al. A strategy of vascular-targeted therapy for liver fibrosis. Hepatology. 2022;76:660–75.
23. Lee KS, Park SJ, Kim SR, Min KH, Lee KY, Choe YH, et al. Inhibition of VEGF blocks TGF-beta1 production through a PI3K/Akt signalling pathway. Eur Respir J. 2008;31:523–31.
24. Lian YG, Zhou QG, Zhang YJ, Zheng FL. VEGF ameliorates tubulointerstitial fibrosis in unilateral ureteral obstruction mice via inhibition of epithelial-mesenchymal transition. Acta Pharmacol Sin. 2011;32:1513–21.
25. Kang DH, Hughes J, Mazzali M, Schreiner GF, Johnson RJ. Impaired angiogenesis in the remnant kidney model: II. Vascular endothelial growth factor administration reduces renal fibrosis and stabilizes renal function. J Am Soc Nephrol. 2001;12:1448–57.
26. Chiba T, Peasley KD, Cargill KR, Maringer KV, Bharathi SS, Mukherjee E, et al. Sirtuin 5 regulates proximal tubule fatty acid oxidation to protect against AKI. J Am Soc Nephrol. 2019;30:2384–98.
27. Chen YT, Jhao PY, Hung CT, Wu YF, Lin SJ, Chiang WC, et al. Endoplasmic reticulum protein TXNDC5 promotes renal fibrosis by enforcing TGFβ signaling in kidney fibroblasts. J Clin Invest. 2021;131:e143645.
28. Zhu H, Liao J, Zhou X, Hong X, Song D, Hou FF, et al. Tenascin-C promotes acute kidney injury to chronic kidney disease progression by impairing tubular integrity via αvβ6 integrin signaling. Kidney Int. 2020;97:1017–31.
29. Liu D, Lun L, Huang Q, Ning Y, Zhang Y, Wang L, et al. Youthful systemic milieu alleviates renal ischemia-reperfusion injury in elderly mice. Kidney Int. 2018;94:268–79.
30. Chen JW, Huang MJ, Chen XN, Wu LL, Li QG, Hong Q, et al. Transient upregulation of EGR1 signaling enhances kidney repair by activating SOX9(+) renal tubular cells. Theranostics. 2022;12:5434–50.
31. Wang J, Sun X, Wang X, Cui S, Liu R, Liu J, et al. Grb2 induces cardiorenal syndrome type 3: roles of IL-6, cardiomyocyte bioenergetics, and Akt/mTOR pathway. Front Cell Dev Biol. 2021;9:630412.
32. Liu J, Kumar S, Dolzhenko E, Alvarado GF, Guo J, Lu C, et al. Molecular characterization of the transition from acute to chronic kidney injury following ischemia/reperfusion. JCI Insight. 2017;2:e94716.
33. Zhang M, Wu L, Deng Y, Peng F, Wang T, Zhao Y, et al. Single cell dissection of epithelial-immune cellular interplay in acute kidney injury microenvironment. Front Immunol. 2022;13:857025.
34. Mohandas R, Dass B, Ejaz AA. Kinetics of vascular endothelial growth factor and endothelin 1 levels in acute kidney injury. Am J Kidney Dis. 2019;74:712–3.
35. Bouchard J, Mehta RL. Angiogenesis markers and recovery from acute kidney injury: a piece of the puzzle? Am J Kidney Dis. 2019;74:12–14.
36. Kang DH, Joly AH, Oh SW, Hugo C, Kerjaschki D, Gordon KL, et al. Impaired angiogenesis in the remnant kidney model: I. Potential role of vascular endothelial growth factor and thrombospondin-1. J Am Soc Nephrol. 2001;12:1434–47.
37. Maciel TT, Coutinho EL, Soares D, Achar E, Schor N, Bellini MH. Endostatin, an antiangiogenic protein, is expressed in the unilateral ureteral obstruction mice model. J Nephrol. 2008;21:753–60.
38. Basile DP, Friedrich JL, Spahic J, Knipe N, Mang H, Leonard EC, et al. Impaired endothelial proliferation and mesenchymal transition contribute to vascular rarefaction following acute kidney injury. Am J Physiol Ren Physiol. 2011;300:F721–33.
39. Lovisa S, Fletcher-Sananikone E, Sugimoto H, Hensel J, Lahiri S, Hertig A, et al. Endothelial-to-mesenchymal transition compromises vascular integrity to induce Myc-mediated metabolic reprogramming in kidney fibrosis. Sci Signal. 2020;13:eaaz2597.
40. LeBleu VS, Taduri G, O'Connell J, Teng Y, Cooke VG, Woda C, et al. Origin and function of myofibroblasts in kidney fibrosis. Nat Med. 2013;19:1047–53.
41. Agarwal R, Duffin KL, Laska DA, Voelker JR, Breyer MD, Mitchell PG. A prospective study of multiple protein biomarkers to predict progression in diabetic chronic kidney disease. Nephrol Dial Transpl. 2014;29:2293–302.
42. Schrijvers BF, Flyvbjerg A, De Vriese AS. The role of vascular endothelial growth factor (VEGF) in renal pathophysiology. Kidney Int. 2004;65:2003–17.
43. Engel JE, Williams ML, Williams E, Azar C, Taylor EB, Bidwell GL, et al. Recovery of renal function following kidney-specific VEGF therapy in experimental renovascular disease. Am J Nephrol. 2020;51:891–902.
44. Qin Z, Li X, Yang J, Cao P, Qin C, Xue J, et al. VEGF and Ang-1 promotes endothelial progenitor cells homing in the rat model of renal ischemia and reperfusion injury. Int J Clin Exp Pathol. 2017;10:11896–908.
45. Leonard EC, Friedrich JL, Basile DP. VEGF-121 preserves renal microvessel structure and ameliorates secondary renal disease following acute kidney injury. Am J Physiol Ren Physiol. 2008;295:F1648–57.
46. Mansour SG, Zhang WR, Moledina DG, Coca SG, Jia Y, Thiessen-Philbrook H, et al. The association of angiogenesis markers with acute kidney injury and mortality after cardiac surgery. Am J Kidney Dis. 2019;74:36–46.
47. Estrada CC, Maldonado A, Mallipattu SK. Therapeutic inhibition of VEGF signaling and associated nephrotoxicities. J Am Soc Nephrol. 2019;30:187–200.